1   TBCD may be a causal gene in progressive neurodegenerative encephalopathy with atypical

2   infantile spinal muscular atrophy

3

4   **Running title:** TBCD variation in atypical SMA and brain atrophy

5

6   Toshio Ikeda[1]*, Akihiko Nakahara[2], Rie Nagano[3], Maiko Utoyama[1], Megumi Obara[1], Hiroshi

7   Moritake[1], Tamayo Uechi[4], Jun Mitsui[5], Hiroyuki Ishiura[5], Jun Yoshimura[6], Koichiro Doi[6], Naoya

8   Kenmochi[4], Shinichi Morishita[6], Ichizo Nishino[7], Shoji Tsuji[5], and Hiroyuki Nunoi[1]

9

10   [1]Division of Pediatrics, Department of Developmental and Urological-Reproductive Medicine

11   Pediatrics, Faculty of Medicine, University of Miyazaki, Miyazaki, 889-1692, Japan

12   [2]Department of Pediatrics, National Hospital Organization Miyazaki Hospital, Miyazaki, 889-1301,

13   Japan

14   [3]Department of Pediatrics, Aisenkai Nichinan Hospital, Miyazaki, 887-0034, Japan

15   [4]Frontier Science Research Center, University of Miyazaki, Miyazaki, 889-1692, Japan

16   [5]Department of Neurology, The University of Tokyo, Graduate School of Medicine, Tokyo,

17   113-8655, Japan

18   [6]Department of Computational Biology and Medical Sciences, Graduate School of Frontier

19   Sciences, The University of Tokyo, Chiba, 277-8568, Japan

20   [7]Department of Neuromuscular Research, National Institute of Neuroscience, National Center of

1   Neurology and Psychiatry, Tokyo, 187-8551, Japan

2   * Correspondence to: toshio_ikeda@med.miyazaki-u.ac.jp

1   **Abstract**

2   Spinal muscular atrophy (SMA) is an autosomal recessive neurodegenerative disorder caused by

3   survival motor neuron gene mutations. Variant forms of SMA accompanied by additional clinical

4   presentations have been classified as atypical SMA and are thought to be caused by variants in as

5   yet unidentified causative genes. Here, we present the clinical findings of two siblings with an

6   SMA variant followed by progressive cerebral atrophy, and the results of whole exome sequencing

7   analyses of the family quartet that was performed to identify potential causative variants. We

8   identified two candidate homozygous missense variants, R942Q in the tubulin-folding cofactor D

9   gene (*TBCD*), and H250Q in the bromo-adjacent homology domain and coiled coil-containing 1

10   gene (*BAHCC1*), located on chromosome 17q25.3 with an interval of 1.4 Mbp. *In silico* analysis of

11   both variants suggested that *TBCD* rather than *BAHCC1* was likely the pathogenic gene (*TBCD*

12   sensitivity, 0.68; specificity, 0.97; *BAHCC1* sensitivity, 1.00; specificity, 0.00). Thus, our results

13   show that *TBCD* is a likely novel candidate gene for atypical SMA with progressive cerebral

14   atrophy. *TBCD* is predicted to have important functions on tubulin integrity in motor neurons as

15   well as on the central nervous system.

16   **Keywords**: Spinal muscular atrophy, Atypical, Cerebral atrophy, Tubulin-folding cofactor D,

17   Bromo-adjacent homology domain and coiled coil-containing 1, Whole exome family quartet

18   analysis

19

1   **Introduction**

2   Infantile spinal muscular atrophy (SMA) is a frequent autosomal disease that specifically affects the

3   motor neurons of the spinal anterior horn and lower cranial nerve nuclei.[1,2] Peripheral nerve

4   involvement or other organ malformations are conventionally regarded as exclusion criteria for

5   infantile SMA. However, recent reports indicate that although the neurological features are obvious

6   early in childhood, the somatic features appear later in childhood, suggesting an apparent lack of

7   boundaries between purely neurological and multiorgan syndromes over time.[1-3] SMA is caused by

8   mutations in the survival motor neuron genes 1 and 2 (*SMN1* and *SMN2*) on chromosome 5q13.[4]

9   The homozygous absence of *SMN1* is responsible for SMA, whereas *SMN2* copy number is

10   associated with the SMA phenotype.[4]

11   Atypical forms of the disease have been described. Patients with these forms have unusual

12   additional neurological features (e.g., diaphragmatic palsy) that are known as atypical SMA, SMA

13   variant, non-5q-SMA entities, or SMN1-negative proximal SMA.[5–8] Based on the mode of

14   inheritance and involvement of other organs or peripheral nerves, atypical SMA types have been

15   reported along with the causative genes, including pontocerebellar hypoplasia (PCH) with infantile

16   SMA (PCH1A, *VRK1*; PCH1B, *EXSOC3*), SMA and progressive myoclonic epilepsy (PMESMA,

17   *ASAH1*), and SMA with cranial nerve disorders.[5-13]

18   Progressive loss of neurological function along with the involvement of the central nervous system

19   other than the motor neuron system is diagnosed as a neurodegenerative disease and is classified

20   into five major categories: polioencephalopathies, leukoencephalopathies, corencephalopathies,

1   spinocerebellopathies, and diffuse encephalopathies.

2   Here, we present two cases, siblings, who showed symmetrical proximal neurogenic muscle

3   atrophy complicated by cognitive dysfunction and progressive cerebral atrophy. We investigated

4   the possibility that these siblings were affected by atypical SMA with autosomal recessive

5   inheritance. To this end, we conducted whole exome sequencing analyses on the two affected

6   siblings and their parents, identifying variants in the tubulin-folding cofactor D gene (*TBCD*) and

7   the bromo-adjacent homology domain and coiled coil-containing 1 gene (*BAHCC1*) located on

8   chromosome 17q25.3 with an interval of 1.4 Mbp. Our results suggested that *TBCD* was the likely

9   causative variant for these sibling cases.

10

1   **Materials and methods**

2   **Ethics**

3   All studies were performed with the informed consent of the patients' parents and the approval of

4   the Institutional Review Boards at the University of Miyazaki and the University of Tokyo.

5

6   **Participants**

7   Two Japanese familial patients with atypical SMA were enrolled in this study. Their pedigree chart

8   is shown in Figure 1. The detailed clinical features of the sibling cases are provided in the Results

9   section. Their parents were non-consanguineous.

10

11   **Exome sequencing**

12   Genomic DNA was extracted using standard protocols from peripheral blood leukocytes or the

13   umbilical cord of the two patients and their parents. Whole exome sequencing and bioinformatics

14   analysis were performed on the two patients (cases 1 and 2) as previously described.[14,15] Briefly,

15   exonic sequences were enriched using a SureSelect v4+UTRs kit (Agilent, CA) and subjected to

16   massively parallel sequence analysis using an Illumina HiSeq 2500 sequencing system (Illumina,

17   CA). The Burrows–Wheeler Aligner[16] and SAMtools[17] programs were used with the default

18   parameter settings for alignment of raw reads and variation detection (human GRCh37/hg19).

19   Single nucleotide variants were filtered using 800 Japanese, in-house, healthy control exome data

20   collected at the University of Tokyo.

1

2   **SNP genotyping**

3   Genotyping of single nucleotide polymorphisms (SNPs) were performed using a Genome-Wide

4   SNP Array 6.0 (Affymetrix). The availability of genomic DNA enabled genotyping of the genomic

5   DNA of one patient (case 1) and the parents. SNP calling was performed using Genotyping

6   Console software (Affymetrix). PLINK software was used to obtain a pairwise identity-by-descent

7   (IBD) estimation.[18]

8

9   **Sanger sequencing**

10   Sanger sequencing was performed to validate each candidate variant detected by exome

11   sequencing. The entire exon 31 from *TBCD* was amplified by polymerase chain reaction (PCR)

12   using an appropriate primer pair, TBCD-F 5′-GCATGTCCTCGTGGTGCTTG-3′ and TBCD-R

13   5′-GCCAATGATCTCGCCATGGC-3′, and AmpliTaq Gold (Life Technologies Japan, Tokyo,

14   Japan). Similarly, the portion of exon 5 from *BAHCC1* harboring another candidate mutation was

15   amplified by PCR using an appropriate primer pair, BAHCC1-F

16   5′-GAGTCAGTGCCAGCTGGTGTC-3′ and BAHCC1-R

17   5′-CTGCTGCCTCCTTGCACAG-3′ and AmpliTaq Gold.

18   Direct nucleotide sequence analysis was performed using the BigDye Terminator v3.1 kit and an

19   ABI PRISM 3130 Genetic Analyzer instrument (Life Technologies Corporation, Carlsbad, CA,

20   USA).

1

2   **Database analyses**

3   Sequences were compared with wild-type sequences using the online Basic Local Alignment

4   Search Tool (BLAST; http://blast.ncbi.nlm.nih.gov/Blast.cgi) and the National Center for

5   Biotechnology Information (NCBI) database (http://www.ncbi.nlm.nih.gov/homologene). Variants

6   were tested for potential pathogenicity using the following bioinformatics software online tools:

7   Polymorphism Phenotyping v2 (PolyPhen2; http://genetics.bwh.harvard.edu/pph2/index.shtml),

8   Scale-Invariant Feature Transform (http://sift.jcvi.org/), and Align GVGD

9   (http://agvgd.hci.utah.edu).[10,19-20] Protein structure predictions were performed using JPred 4

10   (http://www.compbio.dundee.ac.uk/jpred/) and I-TASSER

11   (http://zhanglab.ccmb.med.umich.edu/I-TASSER/).[21,22]

12

1 **Results**

2 Case reports

3 Case 1: A 1-month-old girl was referred to our hospital with hypotonia and developmental

4 problems. She was the first child of unrelated, healthy Japanese parents (Fig. 1) and was born

5 weighing 3,080 g at 38 weeks' gestation via uterine inertia without fetal and neonatal hypoxemia.

6 Her vital signs and weight gain were normal, but she exhibited a frog-leg posture and head lag. She

7 had no dysmorphic facial features or hepatosplenomegaly. Her mental status was alert and she was

8 visually attentive. She cried weakly. Her eye positions were normal, there were no ocular deviations,

9 and her pupils were equal, round, and reactive to light. Her face moved symmetrically. She was

10 able to swallow during the initial visit. A high-arched palate was not noted. The tongue was midline

11 and fasciculations were suspected. She had almost normal bulk with marked hypotonia. The Scarf

12 sign was positive, with diffuse muscle weaknesses encompassing the trunk, limb symmetries, and

13 proximal muscle dominance. She was unable to lift her arms or legs against gravity, but had some

14 movement of her hands and feet. Facial muscular weakness was noted. Pes equinus of both feet

15 was noted. Involuntary movements were not observed. She exhibited some withdrawal and

16 grimacing to pain. Although bilateral plantar flexor responses were absent, the Babinski reflex was

17 positive, showing contraction of the extensor hallucis longus muscle. The Moro reflex was positive

18 but weak. At her first visit, serum biochemical markers (creatine kinase, lactate, pyruvate, amino

19 acid levels, and other blood serology) were in the normal range. Brain magnetic resonance imaging

20 (MRI) (Fig. 2a) results showed no obvious abnormal signal. No deletions or mutations in exons 7

1   and 8 of the *SMN* gene were identified from nucleotide sequence analyses of the PCR products,

2   excluding typical infantile SMA.

3   At 3 months of age, tongue fasciculations were clearly apparent, and her voluntary smile and visual

4   attention were lost. She was admitted again at 7 months due to a failure to thrive. Cerebral atrophy

5   was confirmed by a computed tomography (CT) scan and also by brain MRI (Fig. 2b), with no

6   findings of cerebellar atrophy or brainstem changes. Her head circumference was 0.23 SD at 1

7   month, but -2.1 SD at 8 months. Psychomotor retardation was clearly apparent and progressive.

8   Symptomatic partial seizure was observed, which was intractable to antiepileptic drugs. In addition

9   to a weak cough and cry, respiratory distress and dysphagia with a bell-shaped chest and

10   paradoxical respirations were confirmed at 9 months of age. She began to have difficulty

11   swallowing. By 12 months she was profoundly mentally and physically retarded, with a

12   developmental quotient less than 20. She was confined to bed, lost spontaneous movements,

13   communication, or interaction with the environment, and she needed continuous tracheotomy

14   positive-pressure ventilation and tube nutrition. Although mild optic atrophy was observed, macular

15   cherry-red spots and retinal pigmentary changes were not noted. Pupil responses, eye positions, and

16   ocular movements were normal, but reaction to light became incomplete. Optokinetic nystagmus,

17   pursuit, saccade, and eye contact were lost. These findings indicated progressively deteriorating

18   visual functions, especially due to cortical visual impairment. Click-evoked auditory brainstem

19   response (ABR) thresholds at 9 months of age were 30 dB nHL (right) and 40 dB nHL (left).

20   Latencies of waves I (right 1.68 ms, left 1.54 ms; normal 1.60 ± 0.46), Ⅲ (right 3.70 ms, left 3.48

1   ms; normal 4.30 ± 0.50), and Ⅴ (right 6.12 ms, left 5.28 ms; normal 6.63 ± 0.78) were obtained

2   using 90 dB high-click stimuli at 9 months. These findings indicated normal auditory peripheral

3   nerve and brainstem functions.

4   Reduced nerve conduction velocity (27 m/sec; normal 42.3 ± 6.4) and reduced compound muscle

5   action potential (2.5 mV; normal 5.5 ± 2.0) were observed in the median nerve. Reduced nerve

6   conduction velocity (24 m/sec; normal 38.5 ± 5.5) and reduced compound muscle action potential

7   (0.93 mV; normal 14.1 ± 2.6) were also observed in the posterior tibial nerve (Fig. 2d).

8   Lysosomal enzyme activities that are relevant to neurodegeneration involving the central nervous

9   system and hypotonia (e.g., glycosidases, lysosomal proteases, and sulfatases) were in normal

10 ranges. Normal serum levels of very long chain fatty acids excluded fatty acid beta oxidation cycle

11 disorders, medium-chain acyl-coenzyme A dehydrogenase deficiency, long chain

12 3-hydroxyacyl-coenzyme A dehydrogenase deficiency, very long chain acyl-coenzyme A

13 dehydrogenase deficiency, and glutaric acidemia type II. G-banded chromosomal analysis was

14 normal. Cardiovascular, hepatic, and renal functions were also normal. Echocardiography showed

15 no signs of cardiomyopathy. At 3 years of age, a muscle biopsy specimen confirmed large grouped

16 atrophy with fiber hypertrophy (Fig. 2e). Sural nerve biopsy was normal upon optical microscopic

17 examination (Fig. 2f). She died of aspiration pneumonia at 6 years of age.

18

19 Case 2: The second patient was the younger sister of case 1 (Fig. 1). She was born at 39 weeks'

20 gestation via normal delivery without fetal and neonatal hypoxia, and weighed 3,060 g. She was

1   referred to our hospital at 6 months of age with hypotonia, developmental problems, and pes

2   equines. Her vital signs and weight gain were normal, but she exhibited a frog-leg posture and head

3   lag. At the initial visit, her head circumference was within the normal range but became smaller

4   than the reference range with increasing age. Her tongue was midline with fasciculations. Her

5   respiratory condition, mental status, other symptoms, and sensory and reflex responses were the

6   same as those described for her sister. She also had severe psychomotor retardation. Intractable

7   symptomatic partial seizure occurred at 8 months. Respiratory distress and dysphagia were

8   progressive, and she needed a tracheostomy at 7 months. She has been mechanically ventilated to

9   date, and is currently bedridden with profound mental retardation. She is still alive at the age of 7

10   with tracheotomy positive-pressure ventilation, home-based respirator care.

11   Her serum biochemical markers were normal. Brain MRI showed severe cerebral atrophy (Fig. 2c),

12   but no apparent cerebellar atrophy or brainstem changes. An interictal electroencephalogram

13   showed occasional multi-foci paroxysmal sharp waves on a background activity of dysmorphic

14   high-normal voltage delta and theta waves. This electroencephalogram did not indicate

15   hypsarhythmia. Cardiovascular and hepatic functions were normal. A congenital solitary kidney

16   was detected. At 7 years of age, eyelash and light reflexes were lost. Chromosomal G-band analysis

17   and array comparative genomic hybridization (27K; Agilent Technologies) found no chromosomal

18   abnormality or copy number variations. She has lived a life similar to her elder sister.

19   Differential diagnoses are listed in the Supplementary online material (Supplement 1).

1   **Exome sequence analysis**

2   A total of 142 rare protein-altering and splice-site variants, whose minor allele frequencies (MAFs)

3   were less than 0.5% in 800 exomes from in-house, healthy controls, were identified in one or both

4   cases. All variants in each participant were surveyed for compound heterozygous or homozygous

5   variants that were consistent with an autosomal recessive trait in the family (Table 1).

6   Only two homozygous variants, c.750C>A (H250Q) in *BAHCC1* and c.2825G>A (R942Q) in

7   *TBCD*, at 17q25.3 were shared between the siblings (Table 2). Their parents were heterozygous for

8   the same variants of the alleles. R942Q in *TBCD* was present neither in the exomes from the 800

9   in-house, healthy controls nor in the Exome Aggregation Consortium data set, whereas H250Q in

10   *BAHCC1* was observed in 2 of the 800 in-house, healthy controls (2 in 1,600 alleles) (Fig. 3).

11

12   *In silico* **functional prediction of the variants**

13   PolyPhen2 predicted the *BAHCC1* variant to be benign with a score of 0.000 (sensitivity, 1.00;

14   specificity, 0.00). By contrast, the *TBCD* variant was predicted to be probably damaging, with a

15   score of 0.995 (sensitivity, 0.68; specificity, 0.97). Moreover, Align GVGD predicted the *TBCD*

16   variant as more likely than the *BAHCC1* variant to interfere with function. SIFT predicted both

17   variants to affect protein functions, albeit with a postscript that the substitutions may have been

18   predicted to affect functions because the sequences used were not sufficiently diverse. Protein

19   structure predictions suggested that R942Q in TBCD may affect protein conformations and higher

20   structures of an alpha helix (Fig. 4).

1   **Discussion**

2   The siblings showed atypical SMA at a very early age during childhood, with hypotonia and

3   muscle weakness indicating lower motor unit dysfunction, but, in addition, progressive

4   complicated central nervous system dysfunctions. Severe infantile generalized weakness with

5   tongue fasciculations and respiratory failure suggested an anterior horn disorder, such as SMA. A

6   muscle biopsy specimen at 3 years of age confirmed grouped atrophy of muscles. The results of the

7   nerve conduction study indicated that the tibial nerve showed axonal-dominant degeneration or

8   motor unit reduction, whereas the results of the sural nerve biopsy suggested that the sural nerve

9   was normal, indicating that the pathology was confined to motor neurons. Brain atrophy was

10   progressive. The patient histories indicated severe developmental delay and regression, hypotonia,

11   loss of visual attention, progressive feeding and respiratory problems, and, ultimately, both patients

12   became bedridden and lost any cognitive function at 3 years of age.

13   Progressive diffuse central nervous system disorders with cognitive (i.e., developmental quotient

14   less than 20) and motor dysfunctions are quite different from those observed in typical SMA, and,

15   furthermore, distinct from any other atypical forms of SMA, emphasizing the uniqueness of the

16   clinical presentations of these sibling cases.

17   After differentiating motor neuron diseases from typical SMA and other disorders with similar

18   clinical features, such as infantile hypotonia or psychomotor regression (see Supplement 1), we

19   considered atypical SMA and amyotrophic lateral sclerosis (ALS).[23-26] Additional features,

20   including arthrogryposis, myoclonic epilepsy, sensory neural deafness, or pontocerebellar

1 hypoplasia, were also investigated.[8-27] However, none of these features were observed, and ALS

2 was unlikely, because ALS is usually regarded as an adult-onset neurodegenerative disorder.[27]

3 Many congenital neurodegenerative diseases or atypical SMA are known for distinct diagnoses of

4 SMA1-like congenital illnesses, for example, SMA with respiratory distress (SMARD1), SMA

5 with progressive myoclonic epilepsy (SMAPME), and pontocerebellar hypoplasia (PCH1A,

6 PCH1B).[4-6] The siblings here exhibited some symptoms of SMARD1 (caused by *IGHMBP2*

7 mutations), showing severe respiratory distress at the age of 1 to 6 months, but hemiparalysis of the

8 diaphragm, a characteristic finding of SMARD1, was not observed.[11,28] Furthermore, SMARD1

9 does not complicate central nervous system disorders.[11,28]

10 Pontocerebellar hypoplasia exhibits the most similar clinical course to SMA, and refers to a group

11 of severe neurodegenerative disorders that affect growth and function of the brainstem and

12 cerebellum, eventually resulting in little or no development.[8,29,30] Different types of pontocerebellar

13 hypoplasia are classified based on clinical findings and the spectra of pathological changes.[8,29,30]

14 Type 1 PCH is characterized by central and peripheral motor dysfunction associated with anterior

15 horn cell degeneration, and resembles infantile SMA, usually leading to early death.[29,30] With type

16 2 PCH, there is progressive microcephaly from birth combined with extrapyramidal

17 dyskinesias.[29,30] Marked PCH and progressive cerebral atrophy are revealed by brain CT. Here, the

18 siblings showed microcephaly, progressive cerebral atrophy (but not spastic palsy), severe

19 extrapyramidal dyskinesia, and failure to acquire any voluntary skills. There are many other types

20 of PCH (2–7), but hyperreflexia, optic atrophy (PCH3), joint contracture, olivopontocerebellar

1   hypoplasia (PCH4), cerebellar hypoplasia apparent in the second trimester, seizures (PCH5), and

2   mitochondrial respiratory chain defects (PCH6) were not confirmed in the present cases.[29,30]

3   Genital abnormalities associated with PCH (PCH7) are only observed in patients with the XY

4   karyotype.[30]

5   To the best of our knowledge, the same clinical presentation observed here has not been previously

6   reported; hence, we conducted exome sequencing of the family quartet: the patients (cases 1 and 2),

7   and their parents. Assuming autosomal recessive inheritance, we searched for genes with

8   compound heterozygous or homozygous protein-altering or splice-site variants with MAFs less

9   than 0.5% in the exomes from the 800 in-house, healthy controls, and found that the siblings

10   carried two homozygous missense variants, R942Q in *TBCD* and H250Q in *BAHCC1*. Their

11   parents had the same variants of these genes in heterozygous states. R942Q in *TBCD* is a novel

12   variant, while H250Q in *BAHCC1* was observed in 2 of the 800 in-house healthy controls,

13   suggesting that R942Q in *TBCD* is more likely than H250Q in *BAHCC1* to be the causative variant.

14   This notion was further supported by the following findings: (1) a variant of *Drosophila TBCD* in

15   projection neurons leads to microtubule destruction and axonal degeneration.[31] (2) Murine *Tbce*

16   gene mutants, homologs of human tubulin-folding cofactor E *(TBCE)*, show phenotypic

17   characteristics of SMA-like motor neuropathy.[32-34] (3) In *Smn*-knockdown cells and SMA-like

18   mice, microtubule density and beta-tubulin levels are reduced.[35] The alpha/beta tubulin heterodimer

19   formation requires participation of a series of chaperone proteins (tubulin-folding cofactors A–E)

20   that function downstream of cytosolic chaperonin as a heterodimer assembly machine, and of

1   which, TBCD forms one of the assemblies.[36] The efficiency with which TBCD affects tubulin

2   disruption *in vivo* depends on its origin: overexpression of bovine TBCD efficiently destroys

3   tubulin and microtubules in cultured cells.[36] Interestingly, TUBA4A has recently been reported to

4   be associated with familial ALS, supporting that tubulin integrity is essential in motor neurons.[37] (4)

5   Additionally, in many syndromes of conventionally grouped purely neurological disorders,

6   extraneurological or other neurological complications will appear later in childhood.[2,3] Giant axonal

7   neuropathy (GAN), related to GAN (gigaxonin) mutations, is known as one of the most

8   recognizable neurodegenerative disorders.[3] GAN controls vimentin organization through a tubulin

9   chaperone (TBCB, TBCE)-independent pathway.[38] Although our cases differed from GAN

10   because of our peripheral nerve biopsy findings, these reports may indicate a relationship between

11   tubulin chaperones and neurodegenerative disorders.

12   According to the protein structure models of Pymol (http://www.pymol.org/) and predicted protein

13   structures, R942 is involved in protein–protein interactions in structured helices,[39,40] and

14   evolutionally conserved among species (Fig. 3). The R942Q variant is suspected to influence

15   protein conformation and function by changing a positive to a neutral amino acid on the protein

16   surface (Fig. 4).

17   While R942Q has not been reported in public databases, two missense changes involving adjacent

18   residues have been annotated (rs753751532, H941Y; rs8072406, G943V).[40] The reasons why

19   H941Y and G943V have been reported as not affecting pathogenesis may be that H941Y does not

20   form a helical structure (Fig. 4) and possibly does not highly affect protein structure,[41] and G943V

1 does not alter charged amino acids. Both glycine and valine are nonpolar hydrophobic amino

2 acids.[41] Therefore, we predict that R942Q causes the loss of the electrostatic stability of the TBCD

3 protein due to the alteration from a positive to a neutral charge in an amino acid.[42]

4 The *BAHCC1* gene may also be causative in our cases because mice with a knockout of the human

5 *BAHCC1* ortholog (KIAA 1447) have overt motor deficits.[43] However, *in silico* amino acid

6 prediction analyses of both homologous missense mutations using PolyPhen2 and Align GVGD

7 showed that R942Q in *TBCD* was more likely (sensitivity, 0.68; specificity, 0.97) than H250Q in

8 *BAHCC1* (sensitivity, 1.00; specificity, 0.00) to be causative.[18,44] Guidelines for using prediction

9 methods recommend the application of several tools, if possible. Herein, we analyzed the results

10 using three different prediction tools.[45]

11 *TBCD* and *BAHCC1* are both located on chromosome 17q25.3 at an interval of 1.4 Mbp.

12 Moreover, there is a run of homozygosity in the 1.8 Mbp region (chr17 79,429,228-qter) that

13 includes *TBCD* and *BAHCC1* as observed by exome and high-density SNP results (data not

14 shown), which raised the possibility that both parents inherited the variants in *TBCD* and *BAHCC1*

15 from a common ancestral individual. IBD estimation of the parents from the SNP data, however,

16 did not suggest that the parents were closely related, because the pi-hat value, which estimates the

17 proportion of IBD between them, was 0.0075. Although R942Q in *TBCD* is most likely the

18 causative variant, as discussed above, we cannot rule out the possibility of more complex models

19 (i.e., *TBCD* and *BAHCC1* co-expression, or autosomal dominant transmission due to parental

20 germinal mosaicism). Further functional analyses using *in vivo* and *in vitro* models will be

1   necessary to investigate how these mutations are involved in the clinical presentation.

2   Recently, three papers describing the similar cases with *TBCD* variation were published.[46-48] The

3   patients of these papers were described as early-onset cortical atrophy, postnatal microcephaly, and

4   developmental delay/regression.[46-48] Several cases appeared postnatal growth retardation, muscle

5   weakness/atrophy, respiratory failure, seizures, optic nerve atrophy, progressive spasticity, or severe

6   dystonia.[46-48] But our cases would be most severe neurodegenerative conditions as in our paper.

7   These papers include some functional aspects of the linkage between the disease phenotype and

8   *TBCD* variation, and they determined *TBCD* as a causal gene of their patients' disease because the

9   phenotypes were quite similar to that of previous report.[46-48]

10   In conclusion, a homozygous mutation in *TBCD*, which encodes tubulin cofactor, is likely

11   responsible for a novel and severe neurodegenerative disorder.

12

1   **Accession numbers and reference sequences**

2   Note: Nucleotide sequence data reported are available in the DNA Data Bank of Japan database

3   under the accession numbers LC071985 and LC072713.

4

5   Reference sequences are available from NCBI for the *Homo sapiens TBCD* mutation

6   (NC_000017.10 chromosome 17 reference GRCh primary Assembly; NC_000017.11

7   chromosome 17 reference GRCh primary Assembly; and NCBI Reference Sequence:

8   NG_011721.1), and the *BAHCC1* mutation (NC_000017.10 chromosome 17 reference GRCh

9   primary Assembly; and NC_000017.11 chromosome 17 reference GRCh primary Assembly).[49]

10

11   **Abbreviations**

12   Spinal muscular atrophy (SMA)

13   survival motor neuron gene (SMN)

14   pontocerebellar hypoplasia (PCH)

15   tubulin-folding cofactor D gene (TBCD)

16   single nucleotide polymorphisms (SNPs)

17   identity-by-descent (IBD)

18   polymerase chain reaction (PCR)

19   bromo-adjacent homology domain and coiled coil-containing 1 gene (BAHCC1)

20   magnetic resonance imaging (MRI)

1   computed tomography (CT)

2   standard deviation (SD)

3   decibel above normal adult hearing level (dB nHL)

4   minor allele frequency (MAF)

5   amyotrophic lateral sclerosis (ALS)

6   Spinal muscular atrophy with respiratory distress type 1 (SMARD1)

7   SMA with progressive myoclonic epilepsy (SMAPME)

8   popliteal fossa (Pop Fossa)

9   latency (LAT)

10   duration (DUR)

11   amplitude (AMP)

12   conduction velocity (CV)

13   microvolt (μV)

14   millisecond (ms)

15

16   **Authors' Contributions**

17   TI confirmed the diagnosis in each participating patient, conceived of the study, participated in the

18   sequence alignment, designed and performed the experiments, analyzed the data, contributed

19   reagents/materials/analysis tools, and drafted the manuscript. AN confirmed the diagnosis for the

20   participating patient designated as case 2, conceived of the study, participated in the sequence

1   alignment, designed and performed the experiments, analyzed the data, and helped to draft the

2   manuscript. RN confirmed the diagnosis for the participating patient designated as case 1. MU

3   performed the experiments. MO designed and performed the experiments, and analyzed the data.

4   HM conceived of the study and helped to draft the manuscript. TU conceived and designed the

5   experiments. JM performed the experiments and contributed reagents/materials/analysis tools. HI

6   performed the experiments and contributed reagents/materials/analysis tools. JY performed the

7   experiments and contributed reagents/materials/analysis tools. KD performed the experiments and

8   contributed reagents/materials/analysis tools. NK conceived and designed the experiments. SM

9   performed the experiments and contributed reagents/materials/analysis tools. NI conceived and

10   designed the experiments. ST conceived and designed the experiments and contributed

11   reagents/materials/analysis tools and drafted manuscript. HN conceived of the study, and

12   participated in its design and coordination and helped to draft the manuscript. All authors read and

13   approved the final manuscript.

14

15   **Conflicts of Interest**

1

Supplementary information is available on the website for *Journal of Human Genetics*.

References

1. Rudnik-Schöneborn, S., Goebel, HH., Schlote, W., Molaian, S., Omran, H., Ketelsen, U. *et al.*

Classical infantile spinal muscular atrophy with SMN deficiency causes sensory neuronopathy.

Neurology. **60**, 983–987 (2003).

2. Pierre, L. & Jonathan, B. Early onset (childhood) monogenic neuropathies. *Handb. Clin. Neurol.*

115, 863-891. doi:10.1016/B978-0-444-52902-2.00049-7 (2013).

3. Pierre, L., Jonathan, B. & Peter D. Hereditary motor-sensory, motor, and sensory neuropathies in

1   childhood. *Handb. Clin. Neurol.* **113**, 1413-1432. doi:10.1016/B978-0-444-59565-2.00011-3.

2   (2013)

3

4   4. Wirth, B. An update of the mutation spectrum of the survival motor neuron gene (SMN1) in

5   autosomal recessive spinal muscular atrophy (SMA). *Hum. Mutat.* **15**, 228–237 (2000).

6

7   5. Ursula, FM., Katja, G., Anja, H., Christine, S., Klaus, Z., Christoph, B. *et al.* Severe spinal

8   muscular atrophy variant associated with congenital bone fractures. *J. Child. Neurol.* **17**, 718–721

9   (2002).

10

11 6. Klaus, Z. & Sabine, RS. 93rd ENMC international workshop: non-5q-spinal muscular atrophies

12 (SMA) – clinical picture (6–8 April 2001, Naarden, The Netherlands). *Neuromuscul. Disord.* **13,**

13 179–183 (2003).

14

15 7. Nathalie, G., Jean-Marie, C., Jean-Christophe, C., Jean-Francois, H., Sylvie, J. & Louis, V. *Brain.*

16 *Dev.* **30**, 169–178 (2008).

17

18 8. Kristien, P., Teodora, C. & Albena, J. Clinical and genetic diversity of SMN1-negative

19 proximal spinal muscular atrophies. *Brain.* **137**, 2879-2896. doi:10.1093/brain/awu169 (2014).

20

1   9. Rudnik-Schöneborn, S., Forkert, R., Hahnen, E., Wirth, B. & Zerres, K. Clinical spectrum and

2   diagnostic criteria of infantile spinal muscular atrophy: further delineation on the basis of SMN

3   gene deletion findings. *Neuropediatrics.* **27,** 8–15 (1996).

4

5   10. Kumar, P., Henikoff, S. & Ng PC. Predicting the effects of coding non-synonymous variants on

6   protein function using the SIFT algorithm. *Nat. Protoc.* **4,** 1073–1081 (2009).

7

8   11. Kaindl, AM., Guenther, UP., Rudnik-Schöneborn, S., Varon, R., Zerres, K., Schuelke, M. *et al.*

9   Spinal muscular atrophy with respiratory distress type 1 (SMARD1). *J. Child. Neurol.* **23,** 199–204

10   (2008).

11

12   12. Grohmann, K., Markus, S., Alexander, D., Katrin, H., Barbara, L., Coleen, A. *et al.* Mutations

13   in the gene encoding immunoglobulin μ-binding protein 2 cause spinal muscular atrophy with

14   respiratory distress type 1. *Nat. Genet.* **29,** 75–77 (2001).

15

16   13. Guenther, UP., Handoko, L., Laggerbauer, B., Jablonka, S., Chari, A., Alzheimer, M. *et al.*

17   IGHMBP2 is a ribosome-associated helicase inactive in the neuromuscular disorder distal SMA

18   type 1 (DSMA1). *Hum. Mol. Genet.* **18,** 1288–1300 (2009).

19

20   14. Ishiura, H., Fukuda, Y., Mitsui, J., Nakahara, Y., Ahsan, B., Takahashi, Y. *et al.* Posterior column

1 ataxia with retinitis pigmentosa in a Japanese family with a novel mutation in FLVCR1.

2 *Neurogenetics.* **12,** 117–121 (2011).

3

4 15. Ishii, A., Saito, Y., Mitsui, J., Ishiura, H., Yoshimura, J., Arai, H. *et al.* Identification of ATP1A3

5 mutations by exome sequencing as the cause of alternating hemiplegia of childhood in Japanese

6 patients. *PLoS. One.* **8,** e56120. doi:10.1371/journal.pone.0056120 (2014).

7

8 16. Heng, L. & Richard, D. Fast and accurate short read alignment with Burrows–Wheeler

9 transform. *Bioinformatics.* **25,** 1754–1760 (2009).

10

11 17. Heng, L., Bab, H., Alec, W., Tim, F., Jue, R., Nils, H. *et al.* The Sequence Alignment/Map

12 format and SAMtools. *Bioinformatics.* **25,** 2078–2079 (2009).

13

14 18. Shaun, P., Benjamin, N., Kathe, TB., Lori, T., Manuel, ARF., David, B. *et al.* PLINK: A Tool

15 Set for Whole-Genome Association and Population-Based Linkage Analyses. *Am. J. Hum. Genet.*

16 **78,** 615–628 (2007).

17

18 19. Adzhubei, IA., Schmidt, S., Peshkin, L., Ramensky, VE., Gerasimova, A., Bork, P. *et al.* A

19 method and server for predicting damaging missense mutations. *Nat. Methods.* **7,** 248–249 (2010).

20

1   20. George, DC., Chakraborty, C., Haneef, SA., Nagasundaram, N., Chen, L., Zhu, H. *et al.*

2   Evolution- and structure-based computational strategy reveals the impact of deleterious missense

3   mutations on MODY 2 (maturity-onset diabetes of the young, type 2). *Theranostics.* **4,** 366–385

4   (2014).

5

6   21. Drozdetskiy, A., Cole, C., Procter, J. & Barton, GJ. JPred4: a protein secondary structure

7   prediction server. *Nucleic. Acids. Res.* **43**, 389-394. doi:10.1093/nar/gkv332 (2015).

8

9   22. Yang, J. & Zhang, Y. I-TASSER server: new development for protein structure and function

10   predictions. *Nucleic. Acids. Res.* **43**, 174-181. doi:10.1093/nar/gkv342 (2015).

11

12   23. Michel, VJ. In Nelson Textbook of Pediatrics, 17th Edition (Richard, EB., Robert, MK. & Hal,

13   BJ.)2029-2035 (Saunders, Philadelphia, PA, USA, 2001).

14

15   24. Gerald, MF. Clinical pediatric neurology Asigns and Symptoms Appriach 4th edn (W.B.

16   Saunders, Philadelphia, PA, USA, 2001).

17

18   25. JEric, PG. Fenichel's Clinical pediatric neurology Asigns and Symptoms Appriach 7th edn

19   (W.B. Saunders, Philadelphia, PA, USA, 2013).

20

1   26. Sasaki, M., Sugai, K. & Inagaki, M. National Center of Neurology and Psychiatry, Department

2   of child neurology, a manual of diagnosis and treatment 3rd edn (shindantochiryousha, Tokyo,

3   Tokyo, Japan, 2015) (Japanease).

4

5   27. Drik, B., Kevin, T. & Martin, RT. Advances in motor neurone disease. *J. R. Soc. Med.* **107**,

6   14-21. doi:10.1177/0141076813511451 (2014).

7

8   28. Matthew, P., Henry, H., Jean, J., Quen, M., Brian, H., Mary, R. *et al.* Severe infantile neuropathy

9   with diaphragmatic weakness and its relationship to SMARD1. *Brain.* **126**, 2682-2692.

10   doi:10.1093/brain/awg278 (2003).

11

12   29. Stephen, MM., Kaashif, AA., Yalda, M., Erin, LM., Millan, SP., David, C. *et al.* Pontocerebellar

13   hypoplasia: review of classification and genetics, and exclusion of several genes known to be

14   important for cerebellar development. *J. Child. Neurol.* **26,** 288-294.

15   doi:10.1177/0883073810380047 (2011).

16

17   30. Yasmin, N., Peter, GB., Bwee,Tien, PT. & Frank, B. Classification, diagnosis and potential

18   mechanisms in Pontocerebellar Hypoplasia. *Orphanet. J. Rare. Dis.* **6,** 50.

19   doi:10.1186/1750-1172-6-50 (2011).

20

1   31. Okumura, M., Sakuma, C., Miura, M. & Chihara, T. Linking cell surface receptors to

2   microtubules: tubulin folding cofactor D mediates Dscam functions during neuronal

3   morphogenesis. *J. Neurosci.* **35,** 1979–1990 (2015).

4

5   32. Martin, N., Jaubert, J., Gounon, P., Salido, E., Haase, G., Szatanik, M. *et al.* A missense

6   mutation in Tbce causes progressive motor neuronopathy in mice. *Nat. Genet.* **32,** 443–447 (2002).

7

8   33. Winnie, C., Wim, W., Martin, P., Karoly, S., Jan, W., Edwin, R. *et al.*

9   Hypoparathyroidism-retardation-dysmorphism syndrome in a girl: a new variant not caused by a

10   TBCE mutation—clinical report and review. *Am. J. Med. Genet.* **140A,** 611–617. (2006)

11

12   34. Don, WC., Koji, Y. & Pascale, B. Gigaxonin controls vimentin organization through a tubulin

13   chaperone-independent pathway. *Hum. Mol. Genet.* **18,** 1384–1394 (2009).

14

15   35. Hsin-Lan ,W., Yuan-Ta, L., Chen-Hung, T., Sue, LC., Hung, L., Hsiu, MH. *et al.* Stathmin, a

16   microtubule-destabilizing protein, is dysregulated in spinal muscular atrophy. *Hum. Mol. Genet.* **19,**

17   1766–1778 (2010).

18

19   36. Guoling, T., Simi, T. & Nicholas, JC. Effect of TBCD and its regulatory interactor Arl2 on

20   tubulin and microtubule integrity. *Cytoskeleton.* **67,** 706–714 (2010).

1

37. Smith, BN., Ticozzi, N., Fallini, C., Gkazi, AS., Topp, S., Kenna, KP. *et al.* Exome-wide Rare

Variant Analysis Identifies TUBA4A Mutations Associated with Familial ALS. *Neuron.* **84,**

324-331 (2014).

5

38. Cleveland, DW., Yamanaka, K. & Bomont, P. Gigaxonin controls vimentin organization

through a tubulin chaperone-independent pathway. *Hum. Mol. Genet.* (e-pub ahead of print January

24 2009 ; doi:10.1093/hmg/ddp044)

39. Grynberg, M., Jaroszewski, L. &Godzik, A. Domain analysis of the tubulin cofactor system: a

model for tubulin folding and dimerization. *BMC. Bioinformatics.* **4,** 46 (2003).

11

40. Groves, MR. & Barford, D. Topological characteristics of helical repeat proteins. *Curr. Opin.*

Struct. Biol. **9,** 383–389 (1999).

14

41. National Center for Biotechnology Information(NCBI). Single Nucleotide Polymorphism

Database (dbSNP) (1998). http://www.ncbi.nlm.nih.gov/SNP/. Accessed 22 May 2016.

17

42. Anders, L., Lars, L., Jure, P., Goran, L., Poul, N. & Morten, K. *Textbook of structural biology*

(World Scientific Pub Co Inc, Toh Tuck Link, Singapore, 2009)

20

1   43. Nakayama, M., Iida, M., Koseki, H. & Ohara, O. A gene-targeting approach for functional

2   characterization of KIAA genes encoding extremely large proteins. *FASEB. J.* **20**, 1718–1720

3   (2006).

4

5   44. Adzhubei, IA., Schmidt, S., Peshkin, L., Ramensky, VE., Gerasimova, A., Bork, P. *et al.* A

6   method and server for predicting damaging missense mutations. *Nat. Methods.* **7,** 248–249 (2010).

7

8   45. Vihinen, M. Guidelines for Reporting and Using Prediction Tools for Genetic Variation

9   Analysis. *Hum. Mutat.* (e-pub ahead of print 18 January 2013; doi:10.1002/humu.22253).

10

11   46. Noriko, M., Ryoko, F., Chihiro, O., Takahiro, C., Masayuki, M., Hiroshi, S. *et al.* Biallelic

12   *TBCD* Mutations Cause Early-Onset Neurodegenerative Encephalopathy. *Am. J. Hum. Genet.* **99,**

13   950–961 (2016).

14

15   47. Elisabetta, F., Marcello, N., Serena, C., Isabelle, T., Margaret, GA., Alessandro, C. *et al.*

16   Biallelic Mutations in *TBCD,* Encoding the Tubulin Folding Cofactor D, Perturb Microtubule

17   Dynamics and Cause Early-Onset Encephalopathy. *Am. J. Hum. Genet.* **99,** 962-973 (2016).

18

19   48. Shimon, E., Guoling, T., Hayley, C., Hannah, V., Linh, N., Saiuj, B. *et al.* Infantile

20   Neurodegenerative Disorder Associated with Mutations in TBCD, an Essential Gene in the Tubulin

Heterodimer Assembly Pathway. *Hum. Mol. Genet.* (e-pub ahead of print 29 August 2016;

doi:10.1093/hmg/ddw292).

49. National Center for Biotechnology Information(NCBI). Gene. (2003)

http://www.ncbi.nlm.nih.gov/gene/. Accessed 12 February 2015.

50. Wolf, NI. & van der Knaap, MS. AGC1 deficiency and cerebral hypomyelination, *N. Engl. J. Med.* **361,** 1997-1998 (2009)

51. University of California San Francisco. Database of Comparative Protein Structure Models

(ModBase) (2009). http://modbase.compbio.ucsf.edu/modbase-cgi/index.cgi. Accessed 15

February 2015.

1   **Titles and legends to figures**

2   Fig. 1. Family pedigree and chromatograms of two *de novo* variants identified in *TBCD* and

3   *BAHCC1*.

4   Participants with available whole exome sequencing analysis are indicated by dots. Data were

5   obtained by Sanger sequencing during the confirmation process. Direct nucleotide sequence

6   analysis confirmed the *TBCD* variant (exon 31, c.2825G>A, R942Q) and the *BAHCC1* variant

7   (exon 4, c.750C>A, H250Q).

8

9   Fig. 2. T1- and T2-weighted brain MR imaging, nerve conduction study, and muscle biopsy.

10   **a**. MRI of case 1 at 1 month of age showing normal findings. **b**. At 7 months, T1- and T2-

11   weighted brain MR images show progression of cerebral atrophy. Given the severe cerebral

12   atrophy and less homogeneous hyperintensity of the white matter seen on T2-weighted imaging,

13   the MRI findings indicate early-onset neurodegenerative disorder, in which impaired formation of

14   myelin results from neuronal dysfunction.[50] **c**. MRI results of case 2 at 6 months of age also reveal

15   progressive cerebral atrophy with less hyperintensity of the white matter. However, this finding

16   does not mean a primary hypomyelination.[50] **d**. Nerve conduction study of case 1 at 9 months of

17   age. The tibial nerve between the ankle and popliteal fossa shows reduced nerve conduction

18   velocity of 24 m/s (normal 38.5 ± 5.5) and reduced compound muscle action potential of 0.93 mV

19   (normal 14.1 ± 2.6). These findings can be accounted for by either axonal-dominant degeneration

20   or motor unit reduction. Pop Fossa, popliteal fossa; LAT, latency (in ms); DUR, duration (in ms);

1 AMP, amplitude (in millivolts, mV); CV, conduction velocity (in meter per second, m/s); μV,

2 microvolt; ms, millisecond. **e**. Biceps muscle biopsy from case 1 at 4 years of age showing large

3 grouped atrophy with fiber hypertrophy, coincident with SMA findings (hematoxylin and eosin

4 staining). **f**. Sural nerve biopsy from case 1 at 4 years of age. This peripheral nerve biopsy specimen

5 shows no axonal degeneration or swollen axons. Myelin sheaths are maintained (toluidine blue

6 staining).

7 Fig. 3. Identification of the putative causative variants in *TBCD* and *BAHCC1*.

8 **a**. Schematic of the *BAHCC1* gene, composed of 28 exons, and of the *TBCD* gene, composed of

9 1,192 amino acids and 39 exons. **b, c**. Partial amino acid sequence alignment reveals that (b) H250
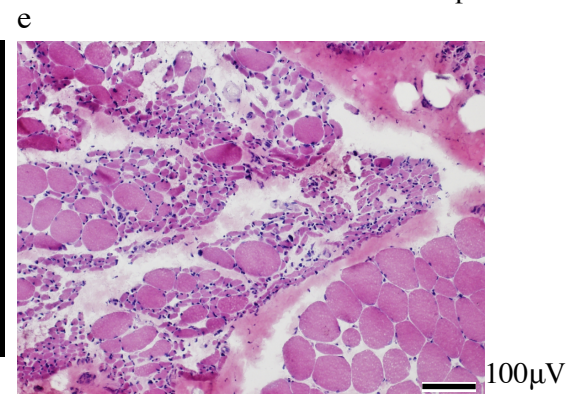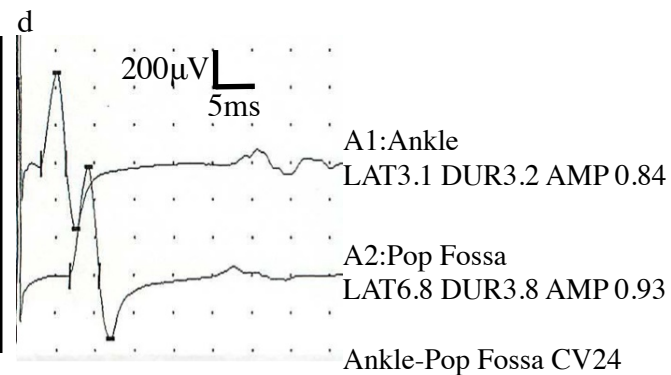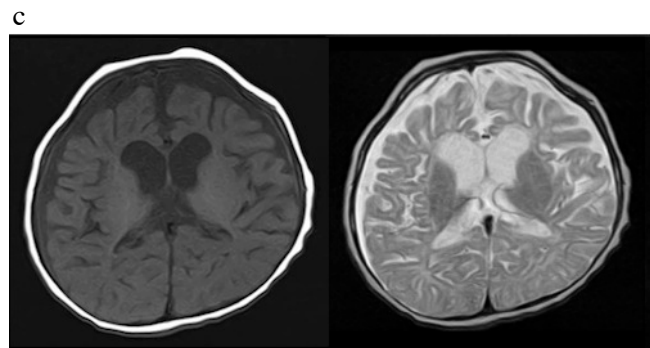
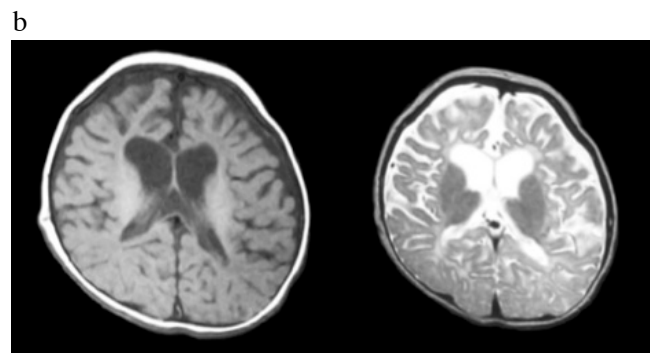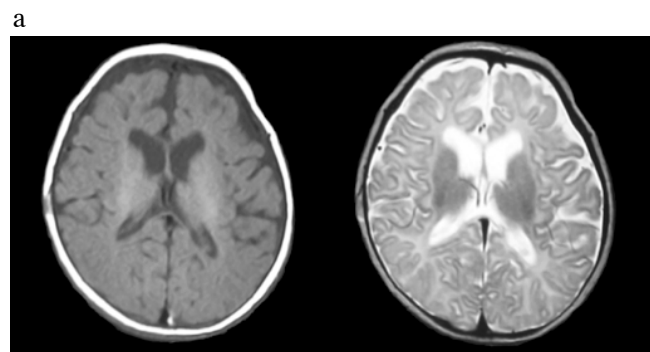10 and (c) R942 are evolutionally conserved among species.

11

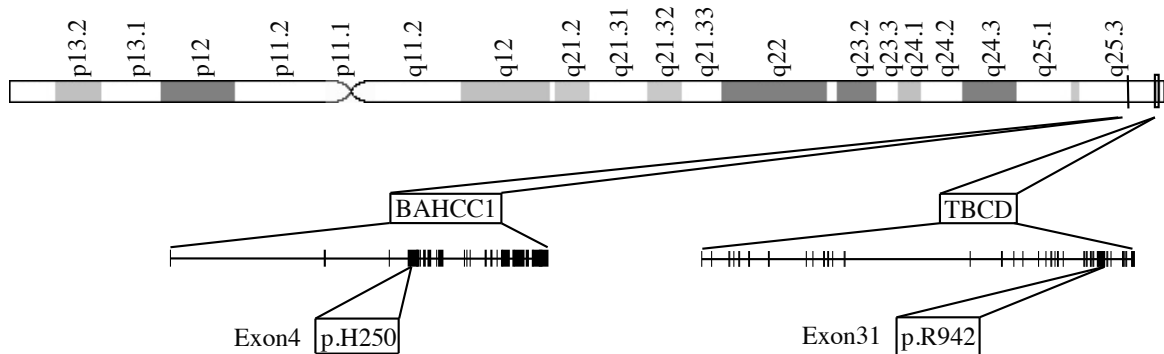12 Fig. 4. Structure models of TBCD showing the R942Q variant.

13 **a, b**. TBCD protein structure from amino acids 865 to 1170; (a) and (b) show the same structures

14 observed at different angles. PBD ID was downloaded using the Mod database.[51] R942Q is located

15 on the protein surface and is part of a helical structure, suggesting it may be involved in protein–

16 protein or intermolecular interactions by causing loss of a positively charged amino acid.[44,50]

17 R942Q is represented using a stick, whereas the other structures are shown as cartoons. **c**. Protein

18 structure predictions using JPred (left) and I-TASSER (right).[22,27] R942Q likely influences an alpha

19 helix. H, alpha helix; C, coil.

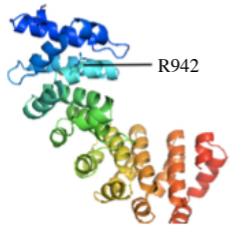|	II-1	II-3	III-2
	G/A	G/A	CACCAAGGA
TBCD R942			
	C/A	C/A	CGGCAAAG
BAHCC1 H250			

a

b

c

d

200μV
5ms

A1:Ankle
LAT3.1 DUR3.2 AMP 0.84

A2:Pop Fossa
LAT6.8 DUR3.8 AMP 0.93

Ankle-Pop Fossa CV24

e

100μV

f

100μV

a. Chromosome17

BAHCC1

TBCD

Exon4 p.H250

Exon31 p.R942
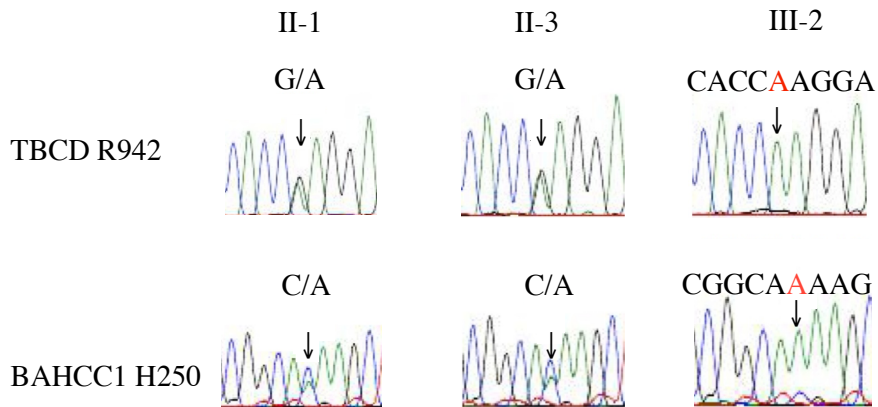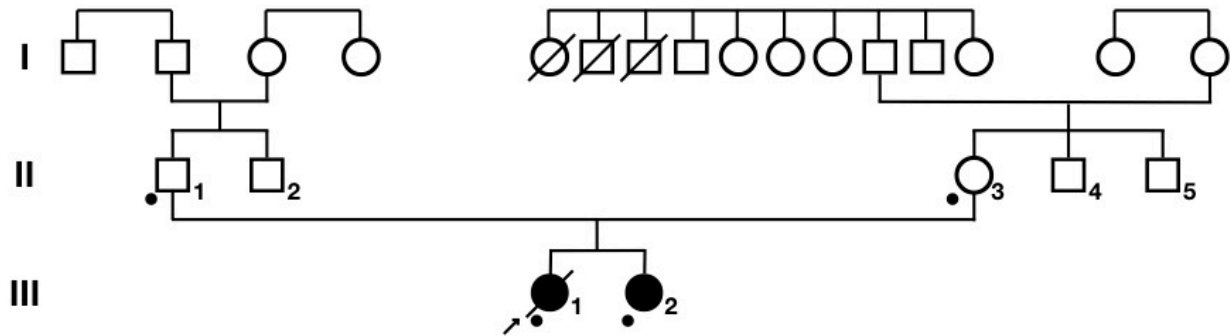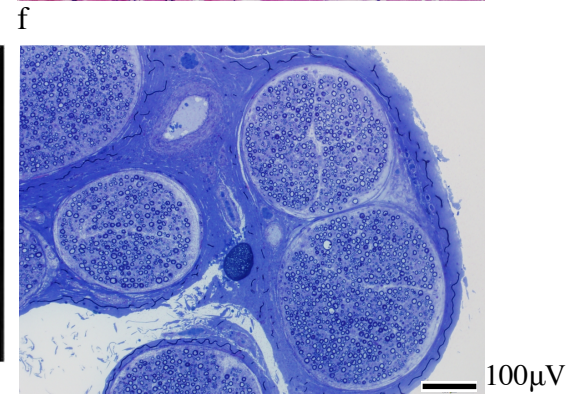
b. BAHCC1 H250Q

Case1 Case2	EDGGKER**Q**KLVLPVPA
Homo sapiens	EDGGKER**H**KLVLPVPA
Macaca mulatta	EDGGKER**H**KLVLPVPA
Canis lupus	DEGGKER**H**KPVLPMPA
Mus musculus	EDSGKDR**Q**KLVPPMPA
Rattus norvegicus	EESSKDR**Q**KLVPPMPA
Gallus gallus	EDDGKER**H**RAVLPVPP
Xenopus tropicalis	LHHHHQH**H**PQHHPQGL
Danio rerio	EDEGKER**Q**KVVLPMSL

c. TBCD R942Q

Case1 Case2	PPIPHVPH**Q**GELEKLFP
Homo sapiens	PPIPHVPH**R**GELEKLFP
Macaca mulatta	PPIPHVPH**R**GELEKLFP
Canis lupus	PPIPHVPH**R**GQLEELFP
Mus musculus	PPIPHVPH**R**QELESLFP
Rattus norvegicus	PPIPHVPH**R**KELESLFP
Gallus gallus	PPVPHIPH**R**EELERIFP
Xenopus tropicalis	PAVPHIPH**H**EELLSIFP
Danio rerio	PRIPYIRE**H**SKLLEIFP

a

b

C

R942
↓
PHVPH**R**GELEKLFPR
| | | | | | | | | | | | | | | |
– – – – – –HHHHHHHH– –

R942
↓
PHVPH**R**GELEKLFPR
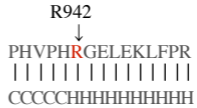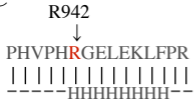| | | | | | | | | | | | | | | |
CCCCCHHHHHHHHHHH
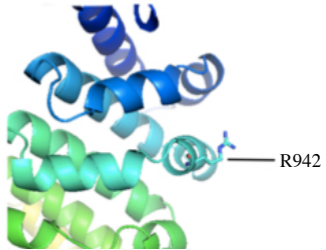
1   Table 1. Novel nonsynonymous variants detected in target regions of case 1 and case 2.

	Reads	Mapped Reads	Mapped Reads (unique)	Mapping Rate (%)	Mapping Rate (unique) (%)	Coverage	Coverage (unique)
Case 1	79,409,125	111,355,984	109,060,264	99.2	97.2	156.3	153.1
Case 2	80,887,120	115,004,732	110,418,648	98.9	95.0	99.4	95.4

4

2　　　Table 2. Candidate homozygous variants detected in case 1 and case 2.

Chromo-Some	Position	Refer-ence	Alter-nation	Zygosity	Mean allele frequency within in house controls	Gene	Amino acid mutation
Chr17	79,409,125	C	A	Homo	2/800(0.25%)	*BAHCC1*	H250Q
Chr17	80,887,120	G	A	Homo	0/800	*TBCD*	R942Q

4

3   Table 3. Predictions on the effect of missense substitutions in *BAHCC1* and *TBCD* .

Gene	Mutation	Polyphen2	SIFT	Align GVGD
BAHCC1	H250Q	Benign	Affects protein function	Class C15[*]
TBCD	R942Q	Probably Damaging	Affects protein function	Class C35[*]

4   *Classifiers are ordered along a spectrum (C0, C15, C25, C35, C45, C55, and C65) from most

5   likely to interfere with function (C65) to least likely (C0).